Lei SUN, Huali WANG, Guangjie XU

College of Communications Engineering, PLA University of Science and Technology

A Real-Valued Direction-of-Arrival Estimation Method Based on Subspace Approximation

Abstract. In this paper, a completely real-valued approach for direction finding is developed. The proposed algorithm using high order powers of the sample covariance matrix to approximate the noise subspace in the real domain, so that the computational burden is substantially reduced and the number of incident sources is not required. Numerical simulation results demonstrate the satisfying performance of the proposed method under various scenarios with uncorrelated or pairwise correlated signals.

*Streszczenie. W artykule przedstawiono metodę wyznaczania kierunku, której działanie opiera się na wyznaczaniu wysokich potęg macierzy kowariancji próbki, w celu aproksymacji podprzestrzeni zakłóceń w dziedzinie rzeczywistej. Pozwala to na redukcję obciążenia obliczeniowego. Nie jest wymagana informacja o ilości źródeł. Przedstawiono wyniki symulacji numerycznych, weryfikujące skuteczność proponowanej metody. (**Metoda wartości rzeczywistych estymacji kierunku w oparciu o aproksymację podprzestrzeni**).*

Keywords: Direction-of-arrival estimation, subspace approximation, unitary transformation.
Słowa kluczowe: estymacja kierunku przybycia, aproksymacja podprzestrzeni, transformacja jednostkowa.

1 Introduction

Direction-of-Arrival (DOA) estimation is a very important topic in array signal processing. Nonparametric subspace methods, such as multiple signal classification (MUSIC) [1], estimation of signal parameters via rotational invariance techniques (ESPRIT) [2], are well-known for high spatial resolution. By making good use of the array geometry, these methods may be further enhanced with reduced computational load. The uniform linear array (ULA) with centro-symmetric configuration is particularly studied, and several excellent algorithms have been developed. The first one, as far as we know, is the Unitary-MUSIC proposed in [3]. Then, Haardt and Nossek presented the method of unitary ESPRIT [4], which completely operates in the real domain. In [5], Pesavento and Gershman introduced a unitary formulation of the root-MUSIC method. Low complexity covariance-based approaches for direction finding are proposed in [6, 7]. In the single snapshot case, Thakre *et al.* improved the effective array aperture via unitary transformation [8]. Recently, the unitary MUSIC algorithm are extended and applied to the electronically steerable parasitic array radiator (ESPAR) antennas to enhance the performance [9]. The previous methods reduce the computational complexity by transforming the receiving data into real domain. Meanwhile, by virtue of the forward-backward averaging, the estimation accuracy is improved since the sample size is virtually doubled. Unfortunately, all these real-valued subspace DOA estimation methods require the exact number of the incident sources to be known *a priori* or at least to be correctly estimated. However, classical information criteria, such as Akaike information criterion (AIC) and minimum description length (MDL), tend to give incorrect estimation of the number of sources underlying some practical scenarios, where the sample size is small and the signal-to-noise ratio (SNR) is low. On the other hand, the Capon beamformer [10], which fails to resolve two closely spaced signals within the Rayleigh cell, exhibits a great advantage that the information of the source number is no longer necessity.

Additionally, the computational load cost by the exact singular value decomposition (SVD) or eigenvalue decomposition (EVD) is very expensive, which may prohibits the use of subspace algorithms in some applications. There exist some methods which estimate the signal or noise subspace without performing exact EVD. For instance, the projection approximation subspace tracking algorithm with deflation (PASTd) [11] and multi-stage Wiener filter (MSWF) [12] can estimate the needed subspace iteratively. Whereas, such efficient algorithms also suffer from determining the number of incident signals. Several subspace approximation methods introduced in [13] are different with those of [11] and [12]. They approximate the subspace by applying rational or power-like methods to the sample covariance matrix, and correspondingly develop some accurate subspace-based DOA estimators. In [14], a cascaded Capon beamformer termed as m-Capon is proposed so as to avoid exact EVD and sources number estimation.

In this paper, concentrating on the receiving array with centro-Hermitian property, a new DOA estimating algorithm requiring only real operations is presented. The proposed method approximates the noise subspace using high order powers of the sample covariance matrix so that the costly EVD is avoided. This approximation method is simpler than those in [13], since no threshold is required to set. Compared with its complex counterpart m-Capon [14], the proposed method is computationally more efficient since it completely performs in the real domain. Moreover, the proposed method can handle pairwise correlated signals directly, while the m-Capon fails to work. The performance of the proposed method is demonstrated via numerical experiments, achieving high resolution comparable with that of unitary MUSIC. However, the proposed method is superior to the unitary MUSIC since the information of source number is no longer required.

The remainder of the paper is organized as follows. In Section 2, after briefly describing the array signal model, the m-Capon method is reviewed. Section 3 presents the proposed method. Section 4 compares the computational complexity of the proposed method with those of some other algorithms. Section 5 carries out computer simulations to evaluate the performance of the proposed method. Finally, Section 6 concludes the whole paper.

2 Background

Consider K narrowband far-field sources from distinct directions impinge on a uniform linear array (ULA), consisting of L ($L>K$) sensors with inter-sensor spacing d. The received complex baseband data at time t can be represented by:

(1) $\qquad \mathbf{y}(t) = \mathbf{A}(\boldsymbol{\theta})\mathbf{s}(t) + \mathbf{n}(t) \quad t=1,2,\ldots,T$

where $\boldsymbol{\theta}=[\theta_1,\theta_2,\ldots,\theta_K]^T$ is the DOAs to be estimated, $\mathbf{y}(t)$ is the complex magnitude vector of the arriving signals, which are assumed to be zero mean wide-sense stationary

stochastic processes, $\mathbf{n}(t)$ is a vector of the additive circular complex Gaussian white noise, which is uncorrelated with the signals, T is the number of snapshots, and $(\bullet)^T$ stands for transpose. The columns of the $L \times K$ array manifold matrix $\mathbf{A}(\boldsymbol{\theta})$ are referred to as array steering vectors with $\mathbf{a}(\theta_k)$ corresponding to the direction θ_k, i.e.,

$$(2) \quad \mathbf{a}(\theta_k) = \left[1, e^{-j2\pi d \sin(\theta_k)/\lambda}, \ldots, e^{-j2\pi d(L-1)\sin(\theta_k)/\lambda} \right]^T$$

where λ represents the wavelength of incident signals. The array covariance matrix is given by:

$$(3) \quad \mathbf{R}_y = E\{\mathbf{y}(t)\mathbf{y}^H(t)\} = \mathbf{A}(\boldsymbol{\theta})\mathbf{R}_s\mathbf{A}^H(\boldsymbol{\theta}) + \sigma_n^2 \mathbf{I}_L$$

where $\mathbf{R}_s = E\{\mathbf{s}(t)\mathbf{s}^H(t)\}$ denotes the signal covariance matrix, and σ_n^2 is the noise variance, $\mathbf{I}_L$ stands for an $L \times L$ identity matrix, and the operator $E\{\bullet\}$, $(\bullet)^H$ denotes expectation and conjugate transpose, respectively. Under the assumption that the signals are uncorrelated with each other, the matrix $\mathbf{R}_s$ will be diagonal with the diagonal elements associated with the average power of incident signals. It is known that the minimum eigenvalue of $\mathbf{R}_y$ is equal to σ_n^2 with multiplicity $L-K$. The EVD of $\mathbf{R}_y$ performs the following form:

$$(4) \quad \mathbf{R}_y = \sum_{i=1}^{L} \gamma_i \mathbf{e}_i \mathbf{e}_i^H = \mathbf{E}_s \boldsymbol{\Lambda}_s \mathbf{E}_s^H + \sigma_n^2 \mathbf{E}_n \mathbf{E}_n^H$$

where the diagonal matrix $\boldsymbol{\Lambda}_s = diag(\gamma_1, \gamma_2, \ldots, \gamma_K)$ contains the K largest eigenvalues sorted in descending order, and the corresponding eigenvectors collected in the matrix $\mathbf{E}_s$ constitute the signal subspace. Similarly, the matrix $\mathbf{E}_n$ contains the $L-K$ eigenvectors that are associated with the eigenvalue σ_n^2, and is called the noise subspace. With (4), it is straightforward to get the following equation:

$$(5) \quad \sigma_n^{2m}\mathbf{R}_y^{-m} = \mathbf{E}_s \boldsymbol{\Lambda}_s' \mathbf{E}_s^H + \mathbf{E}_n \mathbf{E}_n^H$$

where $\boldsymbol{\Lambda}_s' = diag(\sigma_n^{2m}/\gamma_1^m, \sigma_n^{2m}/\gamma_2^m, \cdots, \sigma_n^{2m}/\gamma_K^m)$. It is clear that $\sigma_n^2/\gamma_1 < \sigma_n^2/\gamma_2 < \cdots < \sigma_n^2/\gamma_K < 1$, since σ_n^2 is smaller than the signal eigenvalues. Then as m becomes larger, $\sigma_n^{2m}\mathbf{R}_y^{-m}$ will converge to the projector onto the noise subspace, as:

$$(6) \quad \lim_{m \to \infty} \sigma_n^{2m}\mathbf{R}_y^{-m} = \mathbf{E}_n \mathbf{E}_n^H$$

and the rate of convergence is asymptotically proportional to σ_n^2/γ_K. The significance of (6) is that it provides a way of estimating the noise subspace of the matrix $\mathbf{R}_y$ without computing exact EVD. Furthermore, it is important that the number of incident signals need not be estimated.

In practice, the covariance matrix $\mathbf{R}_y$ is consistently estimated by the sample covariance matrix:

$$(7) \quad \hat{\mathbf{R}}_y = \frac{1}{T} \sum_{t=1}^{T} \mathbf{y}_t \mathbf{y}_t^H$$

Based on (6), one gets the so-called m-Capon method [14], whose output spatial spectrum is:

$$(8) \quad P(\theta) = \prod_{i=1}^{m} \frac{1}{\mathbf{a}^H(\theta)\hat{\mathbf{R}}_y^{-1}\mathbf{a}(\theta)} = \frac{1}{\mathbf{a}^H(\theta)\hat{\mathbf{R}}_y^{-m}\mathbf{a}(\theta)}$$

The peaks of $P(\theta)$ indicate the directions of the incident sources. Ideally, the m-Capon DOA estimator coincides with the well-known MUSIC estimator when m approaches infinity. However, in practice, it is reported that relatively large m may provide satisfying results.

3 Real-valued DOA estimation algorithm

Determining the DOAs of incident signals by calculating (8) and searching the peaks of $P(\theta)$ requires complex operations. In this section, we present an improved and computationally more efficient algorithm only with real operations.

The investigated ULA fits the centro-symmetric criterion obviously, since its elements are located symmetrically with respect to the centre. As a result, the theoretical covariance matrix $\mathbf{R}_y$ shows centro-Hermitian property when all the incident signals are mutually uncorrelated, that is:

$$(9) \quad \mathbf{R}_y = \mathbf{J}_L \mathbf{R}_y^* \mathbf{J}_L$$

where $\mathbf{J}_L$ represents the $L \times L$ permutation matrix with ones across its main anti-diagonal and zeros outside, and $(\bullet)^*$ denotes complex conjugate. Practically, the sample version $\hat{\mathbf{R}}_y$ seldom holds this property due to finite samples effect and signal correlation. And this property is often enforced by means of forward-backward averaging:

$$(10) \quad \begin{aligned} \hat{\mathbf{R}}_{FB} &= (\hat{\mathbf{R}}_y + \mathbf{J}\hat{\mathbf{R}}_y^*\mathbf{J})/2 \\ &= \mathbf{A}\hat{\mathbf{R}}_s^{FB}\mathbf{A}^H + \sigma_n^2 \mathbf{I}_L \end{aligned}$$

The yielding $\hat{\mathbf{R}}_{FB}$ is a centro-Hermitian matrix and can be transformed into a real-valued matrix via a well-designed unitary matrix $\mathbf{Q}_L$:

$$(11) \quad \hat{\mathbf{R}}_r = \mathbf{Q}_L^H \hat{\mathbf{R}}_{FB} \mathbf{Q}_L$$

It is necessary to mention that slight difference in the structure of $\mathbf{Q}_L$ arises between odd and even values of L. When L is even, $\mathbf{Q}_L$ is constructed as following:

$$(12) \quad \mathbf{Q}_L = \frac{1}{\sqrt{2}} \begin{bmatrix} \mathbf{I}_{L'} & j\mathbf{I}_{L'} \\ \mathbf{J}_{L'} & -j\mathbf{J}_{L'} \end{bmatrix}$$

where $L' = L/2$. While for odd values of L, $\mathbf{Q}_L$ is defined as:

$$(13) \quad \mathbf{Q}_L = \frac{1}{\sqrt{2}} \begin{bmatrix} \mathbf{I}_{L'} & \mathbf{0} & j\mathbf{I}_{L'} \\ \mathbf{0}^T & \sqrt{2} & \mathbf{0}^T \\ \mathbf{J}_{L'} & \mathbf{0} & -j\mathbf{J}_{L'} \end{bmatrix}$$

where $L' = (L-1)/2$ and $\mathbf{0} = [0,0,\ldots,0_{L'}]^T$. However, it is proved whether L is odd or even does not affect the final results, in this paper we assume L to be even for simplicity. We note that $\hat{\mathbf{R}}_r$ can be calculated directly based on the sample covariance matrix $\hat{\mathbf{R}}_y$ without forward-backward averaging, via:

$$(14) \quad \hat{\mathbf{R}}_r = \text{Re}[\mathbf{Q}_L^H \hat{\mathbf{R}}_y \mathbf{Q}_L]$$

here, $\text{Re}[\bullet]$ denotes the real part. Calculating $\hat{\mathbf{R}}_r$ through (14) is simpler than using (11), but the computational complexity can be reduced even further by transforming the received complex snapshots into real ones before calculating the sample covariance matrix $\hat{\mathbf{R}}_y$. As stated in [4], we partition the snapshot vector $\mathbf{y}(t)$ at time t as:

$$(15) \quad \mathbf{y}(t) = \begin{bmatrix} \mathbf{y}_u(t) \\ \mathbf{y}_d(t) \end{bmatrix}$$

where both $\mathbf{y}_u(t)$ and $\mathbf{y}_d(t)$ are $L' \times 1$ vector. Consider a transformation $\mathcal{T}$, such that:

$$(16) \quad \mathcal{T}(\mathbf{y}(t)) = \begin{bmatrix} \text{Re}\{\mathbf{y}_u(t) + \mathbf{J}_{L'}\mathbf{y}_d^*(t)\} & -\text{Im}\{\mathbf{y}_u(t) - \mathbf{J}_{L'}\mathbf{y}_d^*(t)\} \\ \text{Im}\{\mathbf{y}_u(t) + \mathbf{J}_{L'}\mathbf{y}_d^*(t)\} & \text{Re}\{\mathbf{y}_u(t) - \mathbf{J}_{L'}\mathbf{y}_d^*(t)\} \end{bmatrix}$$

where $\text{Im}[\bullet]$ denotes the imaginary part. It is seen that the transformed snapshot vector now only contains real

elements and the column is doubled. One can calculate the real covariance matrix $\hat{\mathbf{R}}_r$ by:

$$(17) \qquad \hat{\mathbf{R}}_r = \frac{1}{2T}\sum_{t=1}^{T}\mathcal{T}(\mathbf{y}_t)\mathcal{T}^H(\mathbf{y}_t)$$

Be careful that the number of snapshots now is doubled from T to $2T$. Back to the $\hat{\mathbf{R}}_{FB}$, the EVD can be written as:

$$(18) \qquad \hat{\mathbf{R}}_{FB} = \sum_{i=1}^{L}\lambda_i\mathbf{v}_i\mathbf{v}_i^H = \mathbf{V}_s\boldsymbol{\Gamma}_s\mathbf{V}_s^H + \sigma_n^2\mathbf{V}_n\mathbf{V}_n^H$$

As defined in section 2, the matrices $\mathbf{V}_s$ and $\mathbf{V}_n$ are referred to as the signal subspace and noise subspace, respectively. The diagonal matrix $\boldsymbol{\Gamma}_s$ contains the eigenvalues associated with signals. Based on (11), the inverse of $\hat{\mathbf{R}}_r^m$ is related with that of $\hat{\mathbf{R}}_{FB}$ as:

$$(19) \qquad \begin{aligned} \sigma_n^{2m}\hat{\mathbf{R}}_r^{-m} &= \sigma_n^{2m}\mathbf{Q}_L^H\hat{\mathbf{R}}_{FB}^{-m}\mathbf{Q}_L \\ &= \mathbf{Q}_L^H(\mathbf{V}_s\boldsymbol{\Gamma}_s'\mathbf{V}_s^H + \mathbf{V}_n\mathbf{V}_n^H)\mathbf{Q}_L \\ &= (\mathbf{Q}_L^H\mathbf{V}_s)\boldsymbol{\Gamma}_s'(\mathbf{Q}_L^H\mathbf{V}_s)^H + (\mathbf{Q}_L^H\mathbf{V}_n)(\mathbf{Q}_L^H\mathbf{V}_n)^H \end{aligned}$$

Where $\boldsymbol{\Gamma}_s' = diag(\sigma_n^{2m}/\lambda_1^m, \sigma_n^{2m}/\lambda_2^m, \cdots, \sigma_n^{2m}/\lambda_K^m)$.

Similar to (6), $\sigma_n^{2m}\hat{\mathbf{R}}_r^{-m}$ will converge to the real-valued noise subspace projector when m tends to infinity, since $\sigma_n^2/\lambda_1 < \sigma_n^2/\lambda_2 < \cdots < \sigma_n^2/\lambda_K < 1$, as:

$$(20) \qquad \lim_{m\to\infty}\sigma_n^{2m}\hat{\mathbf{R}}_r^{-m} = (\mathbf{Q}_L^H\mathbf{V}_n)(\mathbf{Q}_L^H\mathbf{V}_n)^H$$

The conventional spatial spectrum of the MUSIC algorithm, using the forward-backward covariance matrix, is given by:

$$(21) \qquad P_{FB}(\theta) = \frac{1}{\mathbf{a}^H(\theta)\mathbf{V}_n\mathbf{V}_n^H\mathbf{a}(\theta)}$$

Simply using (20) and omitting the constant factor σ_n^{2m}, one can get the output spatial spectrum readily:

$$(22) \qquad P_r(\theta) = \frac{1}{\tilde{\mathbf{a}}^H(\theta)\hat{\mathbf{R}}_r^{-m}\tilde{\mathbf{a}}(\theta)}$$

where $\tilde{\mathbf{a}}(\theta)$ is the new steering vector, formulated as:

$$(23) \qquad \tilde{\mathbf{a}}(\theta) = \mathbf{Q}_L^H\mathbf{a}(\theta)$$

Since $\mathbf{a}(\theta)$ is not centro-Hermitian, the resulting $\tilde{\mathbf{a}}(\theta)$ still lies in the complex domain after unitary transformation. We note that the main computational load is cost by searching the peaks of $P_r(\theta)$. Hence, the computational reduction will be not as significant as we expected. However, we find that:

$$(24) \qquad \tilde{\mathbf{a}}(\theta) = \mathbf{a}_r(\theta)e^{-j\pi(L-1)\sin\theta d/\lambda}$$

where:

$$(25) \qquad \begin{aligned} \mathbf{a}_r(\theta) = \sqrt{2}[&\cos(\pi(L-1)d\sin\theta/\lambda), \cdots, \cos(\pi d\sin\theta/\lambda), \\ &\sin(\pi(L-1)d\sin\theta/\lambda), \cdots, \sin(\pi d\sin\theta/\lambda)]^T \end{aligned}$$

Substituting (24) into (22), the output spatial spectrum now becomes:

$$(26) \qquad \begin{aligned} P_r(\theta) &= \frac{1}{\mathbf{a}_r^H(\theta)e^{j\pi(L-1)\sin\theta d/\lambda}\hat{\mathbf{R}}_r^{-m}e^{-j\pi(L-1)\sin\theta d/\lambda}\mathbf{a}_r(\theta)} \\ &= \frac{1}{\mathbf{a}_r^H(\theta)\hat{\mathbf{R}}_r^{-m}\mathbf{a}_r(\theta)} \end{aligned}$$

It is obvious that we can replace $\tilde{\mathbf{a}}(\theta)$ in (22) by $\mathbf{a}_r(\theta)$ without affecting the spatial search function $P_r(\theta)$, just like the one did in [3]. Therefore, searching the peaks of the spatial spectrum requires real operations only. Comparing (8) with (26), it can be concluded that the m-Capon method performs as the complex counterpart of the proposed method. Likewise, we shall point out that the presented real-valued DOA estimator approaches the unitary MUSIC in ideal situation.

4 Complexity analysis and summary of the proposed method

In this section, the proposed real-valued DOA estimator, the unitary MUSIC [3], and the m-Capon [14] are compared in terms of computational complexity.

We investigate the proposed method first. It can be seen that using (16) to transform the complex snapshots to real domain only involves real additions, and therefore the complexity can be neglected. The number of flops required to calculate $\hat{\mathbf{R}}_r$ by (17) is $2TL^2$. The computational load of calculating $\hat{\mathbf{R}}_r^m$ rests with m clearly. Larger value of m theoretically provides a better approximation to the noise subspace at the cost of increased computational load. However, due to limited samples effect, simply using larger m may lead to adverse result. According to the simulation results, we set $m=4$, and therefore the computational cost is about $2L^3$. The inverse of $\hat{\mathbf{R}}_r^m$ can be computed in $2L^3/3$ flops. Jointly taking the spectral searching part into consideration, the total computational cost of the proposed method is about $2TL^2+2L^3/3+2L^3+NL^2$ real flops, where N represents the length of the scanning spatial grid.

For the unitary MUSIC, it requires TL^2 complex flops to calculate the array covariance matrix, and $21L^3+NL(L-K)$ real flops to compute the EVD and spatial spectrum.

For the m-Capon method, based on (8), the overall computational cost is about $TL^2+2L^3/3+2L^3+NL^2$ complex flops, when the m is also set to 4.

It is known that one complex flop is implemented by four real flops in practice. We therefore stress that the complexity of the proposed method is about four times lower than the m-Capon. For small number of signals, the proposed method has computational advantage over the unitary MUSIC.

The implementation of the proposed method is summarized as follows.
Step 1) Transform the complex samples to real via (16).
Step 2) Approximate the noise subspace via (19).
Step 3) Compute the spatial spectrum based on (26).

5 Numerical simulations

We carry out some numerical simulations to evaluate the performance of the proposed DOA estimator, and also compare it with respect to unitary MUSIC [3], Capon [10], and m-Capon [14] algorithms. We consider a 10-element ULA, where the sensors are separated by a half wavelength of the incident signals. Each narrowband signal is generated from a Gaussian distribution with zero mean, and we will investigate scenarios with both uncorrelated and pairwise correlated sources. The additive noise is assumed to be white, both temporally and spatially, and Gaussian distributed with zero mean and variance σ_n^2. We set the power order of the sample covariance matrix to 4 in all the simulations unless specially indicated.

In the first simulation, three equal-power narrowband signals are assumed to impinge on the receiving array from the directions of −40°, −30° and 20°. We take SNR=0dB and $T=100$. It is supposed that the number of the sources is known exactly so that the unitary MUSIC algorithm works in its ideal situation.
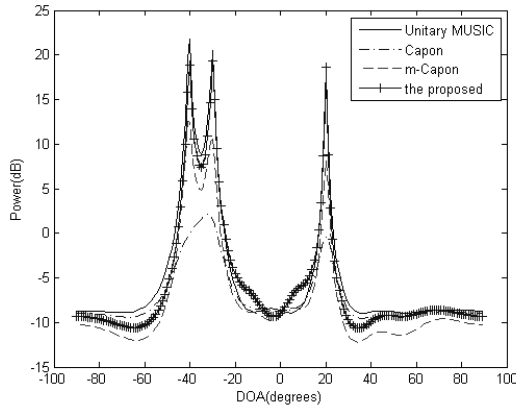
Fig.1(a). Spatial spectra for uncorrelated sources at −40°, −30° and 20°, T=100, SNR=0dB.
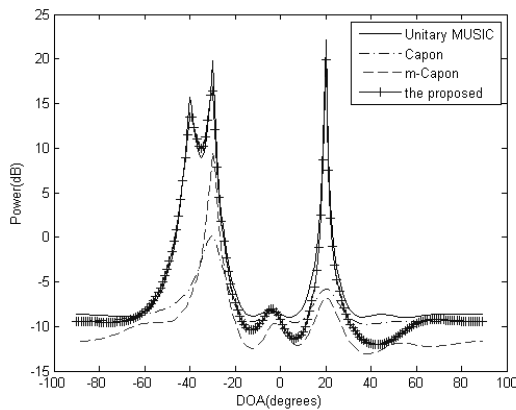

Fig.1(b). Spatial spectra for two coherent sources at −40° and 20°, one uncorrelated source at −30°, T=100, SNR=0dB.

Fig.1 shows the spatial spectra obtained by different algorithms under various conditions. In Fig.1 (a), we show the spatial spectrum plots when the signals are mutually uncorrelated. It is clearly illustrated that the Capon method merges the two closely spaced signals due to the Rayleigh resolution limit. At the same time, the m-Capon and the proposed method are able to distinguish the two as the unitary MUSIC dose. In Fig.1 (b), we show the results when the incident sources at −40° and 20° are coherent but uncorrelated with the one at −30°. Note that both the proposed method and unitary MUSIC succeed in clearly locating the sources, while the Capon and m-Capon fail to work without decorrelation procedure.

In Fig.1, we have provided an intuitionistic comparison between the proposed method and other algorithms. To make the comparison more meaningful, we adopt the average root mean square error (RMSE) to evaluate the statistical DOA estimation performance, defined as:

$$(27) \qquad \text{RMSE} = \sqrt{\frac{1}{K}\sum_{k=1}^{K}\frac{1}{J}\sum_{j=1}^{J}(\hat{\theta}_{kj} - \theta_k)^2}$$

where J=200 for Monte Carlo runs, θ_k denotes the actual arriving angle of the k_{th} signal, while $\hat{\theta}_{kj}$ represents the corresponding estimation in the j_{th} trial.

We investigate the impact of the snapshots and SNR on the RMSE performance of the proposed method and the other three. Three uncorrelated signals with identical SNR impinge on the array from −40°, −30° and 20°. First, we keep the SNR fixed at 5dB and vary the number of

snapshots T. Fig.2 (a) illustrates the RMSE the DOA estimates against the number of snapshots. Then the number of snapshots is fixed, while the SNR varies. Fig.2 (b) shows the estimation RMSE against the SNR when the number of snapshots is kept fixed at 100. From Fig.2, we can conclude that the proposed method provides convincible performance in terms of the estimation RMSE underlying both small sample size and poor SNR scenarios. Among the tested methods, only unitary MUSIC performs slightly better at the cost of higher computational load when the number of incident signals is known exactly.
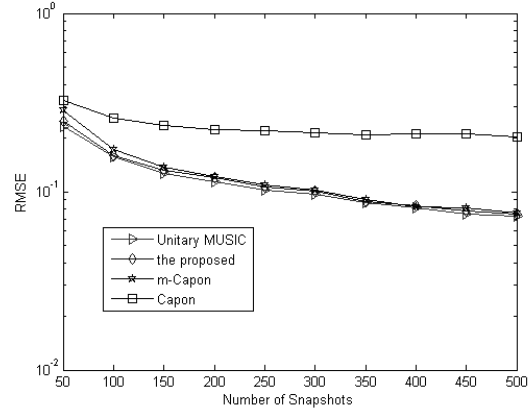

Fig.2(a). RMSE of the DOA estimates versus the number of snapshots T with 5dB SNR.
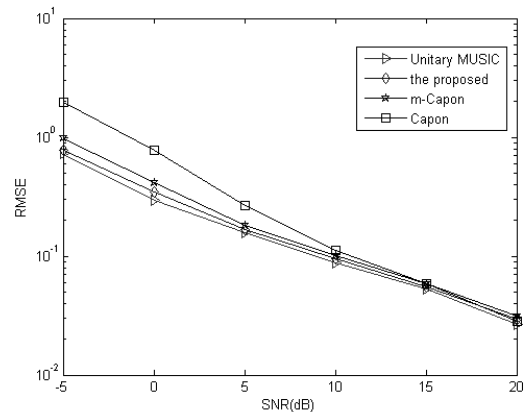

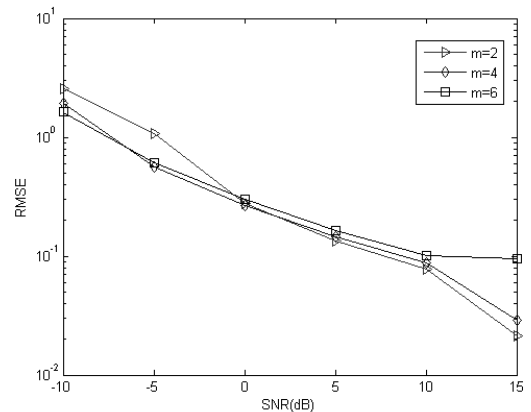Fig.2(b). RMSE of the DOA estimates versus SNR with 100 snapshots.

Fig.3. RMSE of the DOA estimates versus the values of m and SNR with 100 snapshots.

Finally, we examine the impact of the values of m on the RMSE performance of the proposed method. The number of snapshots T=100 and the SNR varies from −10dB to 15dB in a step of 5dB. We simulate two uncorrelated sources located at −40°and −30°. Fig.3 illustrates the estimation RMSE, obtained by the proposed method corresponding to different values of m, as a function of the SNR. It is observed that larger value of m performs better when the SNR is low, while smaller m works better when the SNR is relatively high. This validates that the choice of m=4, which provides satisfying performance in the whole SNR range, is reasonable.

6 Conclusion

In this paper, focusing on the receiving array with centro-Hermitian property, we propose a high resolution DOA estimation method which performs only real operations. Through theoretical analysis and numerical simulations, the estimation performance of the proposed method is confirmed to converge to that of unitary MUSIC asymptotically. However, there are two advantages of the proposed method compared with unitary MUSIC. First, which is more important, the proposed method does not require the knowledge of the number of incident signals. Second, the noise subspace is approximately estimated without calculating exact EVD. Compared with its complex counterpart m-Capon algorithm, the proposed method is computationally more efficient since it operates in real domain completely. Moreover, the proposed method can handle pairwise correlated signals while the m-Capon fails to work. Simulation results have demonstrated the validity and advantages of the proposed method.

REFERENCES
[1] Schmit O.R., Multiple emitter location and signal parameters estimation, *IEEE Trans. Antennas Propag.*, (34)1986, No. 3, 276–280
[2] Roy R., Kailath K., Esprit—Estimation of signal parameter via rotational invariance techniques, *IEEE Trans. Acoust., Speech, Signal Processing*, 37(1989), No. 7, 984–995
[3] Huang K.C., Yeh C.C., A unitary transformation method for angle-of-arrival estimation, *IEEE Trans. Signal Process.*, 39(1991), No. 4, 975-977
[4] Haardt M., Nossek J.A., Unitary ESPRIT: How to obtain increased estimation accuracy with a reduced computational burden, *IEEE Trans. Signal Process.*, 43(1995), No. 5, 1232–1242
[5] Pesavento M., Gershman A.B., Haardt M., Unitary Root-MUSIC with a real-valued eigendecomposition: a theoretical and experimental performance study, *IEEE Trans. Signal Process.*, 48(2000), No. 5, 1306-1314
[6] Ferreira T.N., Netto S.L., Diniz P.S.R., Covariance-based direction-of-arrival estimation with real structures, *IEEE Signal Process. Letters*, 15(2008), 757-760
[7] Ferreira T.N., Netto S.L., Diniz P.S.R., Direction-of-Arrival estimation using a low-complexity covariance-based approach, *IEEE Trans. Aerosp. Electron. Syst*, (48)2012, No. 3, 1924–1934
[8] Thakre A., Haardt M., Giridhar K., Single snapshot spatial smoothing with improved effective array aperture, *IEEE Signal Process. Letters*, (16)2009, No. 6, 505–508
[9] Akkar S., Gharsallah A., Reactance domains unitary MUSIC algorithms based on real-valued orthogonal decomposition for electronically steerable parasitic array radiator antennas, *IET Microw. Antennas Propag.*, (6)2012, Iss. 2, 223–230
[10] Capon J., High resolution frequency-wavenumber spectrum analysis. *Proceedings of the IEEE*, (57)1969, No. 8, 1408-1418
[11] Yang B., Projection approximation subspace tracking, *IEEE Trans. Signal Process.*, (43)1995, No. 1, 95–107
[12] Huang L., Wu S., Feng D., Zhang L., Low complexity method for signal subspace fitting, *Electronics Letters*, (40)2004, No. 14
[13] Hasan M.A., Azimi-Sadjadi M.R., Hasan A.A., Rational invariant subspace approximations with applications, *IEEE Trans. Signal Process.*, 48(2000), No. 11, 3032-3041
[14] Zhang T.L., Liu Y., Liao G.S., Algorithm on high resolution DOA estimation without sources number, *Journal of Electronics & Information Technology*, 30(2008), No. 2, 375-378 (in Chinese)

Authors:
Lei Sun, College of Communications Engineering, PLA Univ. of Sci.&Tech, Biaoying 2, Yudao Street, Nanjing, China, 210007, E-mail: realmufeng@gmail.com;
Prof. Huali Wang, College of Communications Engineering, PLA Univ. of Sci.&Tech,
E-mail:wanghl2008@gmail.com;
Guangjie Xu, College of Communications Engineering, PLA Univ. of Sci.&Tech,
E-mail: moon990@163.com.